Article:

Rougé, C., Tilmant, A., Zaitchik, B.F. et al. (2 more authors) (2018) Identifying key water resource vulnerabilities in data-scarce transboundary river basins. Water Resources Research, 54 (8). pp. 5264-5281. ISSN 0043-1397

https://doi.org/10.1029/2017WR021489

AGU100 ADVANCING EARTH AND SPACE SCIENCE

Water Resources Research

RESEARCH ARTICLE
10.1029/2017WR021489

Key Points:
- This paper presents a two-step framework to identify key vulnerabilities in data-scarce transboundary river basins
- The framework brings together land data assimilation and hydroeconomic analysis to identify these vulnerabilities in complex river networks
- Application to the Tigris-Euphrates basin shows vulnerability of Euphrates portion of basin to additional to irrigation developments

Supporting Information:
- Supporting Information S1

Correspondence to:
C. Rougé,
charles.rouge@gmail.com

Citation:
Rougé, C., Tilmant, A., Zaitchik, B., Dezfuli, A., & Salman, M. (2018). Identifying key water resource vulnerabilities in data-scarce transboundary river basins. *Water Resources Research*, *54*, 5264–5281. https://doi.org/10.1029/2017WR021489

Received 17 SEP 2017
Accepted 30 MAY 2018
Accepted article online 7 JUN 2018
Published online 9 AUG 2018

Identifying Key Water Resource Vulnerabilities in Data-Scarce Transboundary River Basins

Charles Rougé[1,2], Amaury Tilmant[1], Ben Zaitchik[3], Amin Dezfuli[3,4,5], and Maher Salman[6]

[1]Department of Civil Engineering and Water Engineering, Université Laval, Québec City, Québec, Canada, [2]Department of Civil and Environmental Engineering, Cornell University, Ithaca, NY, USA, [3]Department of Earth and Planetary Sciences, The Johns Hopkins University, Baltimore, MD, USA, [4]Global Modeling and Assimilation Office, NASA Goddard Space Flight Center, Greenbelt, MD, USA, [5]Science Systems and Applications, Inc., Lanham, MD, USA, [6]Land and Water Division, Food and Agriculture Organization of the United Nations, Rome, Italy

Abstract This paper presents a two-step framework to identify key water resource vulnerabilities in transboundary river basins where data availability on both hydrological fluxes and the operation of man-made facilities is either limited or nonexistent. In a first step, it combines two state-of-the-art modeling tools to overcome data limitations and build a model that provides a lower bound on risks estimated in that basin. Land data assimilation (process-based hydrological modeling taking remote-sensed products as inputs) is needed to evaluate hydrological fluxes, that is, streamflow data and consumptive use in irrigated agriculture—a lower-end estimate of demand. Hydroeconomic modeling provides cooperative water allocation policies that reflect the best-case management of storage capacity under hydrological uncertainty at a monthly time step for competing uses—hydropower, irrigation. In a second step, the framework uses additional scenarios to proceed with the in-depth analysis of the vulnerabilities identified despite the use of what is by definition a best-case model. We implement this approach to the Tigris-Euphrates river basin, a politically unstable region where water scarcity has been hypothesized to serve as a trigger for the Syrian revolution and ensuing war. Results suggest that even under the framework's best-case assumptions, the Euphrates part of the basin is close to a threshold where it becomes reliant on transfers of saline water from other parts of the basin to ensure irrigation demands are met. This Tigris-Euphrates river basin application demonstrates how the proposed framework quantifies vulnerabilities that have been hitherto discussed in a mostly qualitative, speculative way.

1. Introduction

There are 268 international river basins worldwide, covering about two thirds of the global land mass and hosting about 40% of the world's population (Draper, 2007). The management of those transboundary river basins is challenging due to fragmented and heterogeneous institutions and the sentiment that territorial sovereignty overrides the notion of cooperative basin management (Molle et al., 2007). It took 26 years, starting in 1971, for the international community to come up with a set of principles for sharing water in transboundary river basins, a process which culminated with the adoption of the *UN Convention on the Law of the Non-Navigational Uses of International Watercourses* at the general assembly in 1997 (Wolf, 1999). The first two principles, *equitable and reasonable use* and *obligation not to cause significant harm*, aim at balancing the interests of upstream and downstream countries. The third principle, *the obligation to cooperate*, aims primarily at exchanging hydrological data and information regarding existing and planned future uses in the basin (McCaffrey, 2001).

Data sharing is indeed a prerequisite for cooperation in transboundary river basins (Giuliani & Castelletti, 2013; Watkins, 2006). Yet growing pressure on water resources from riparian countries threatens the validity of cooperative agreements (Kliot et al., 2001) and leads to noncoordinated infrastructure development (e.g., Geressu & Harou, 2015; Tilmant & Kelman, 2007; Tilmant & Kinzelbach, 2012; Wu & Whittington, 2006) with the potential to create closing basins in which available supply can no longer meet rising demands (Mianabadi et al., 2015). Downstream riparians are most at risk then, and their upstream counterparts have little interest in releasing data that would enable crafting policies advocating to share this risk (Timmerman & Langaas, 2005). Therefore, in many transboundary river basins, especially in developing countries, competition over

10.1029/2017WR021489

resource use disrupts data sharing and cooperation, and conversely, fragmentary or nonexistent data about hydrological fluxes hamper the resolution of disputes (Olsson et al., 2010).

This paper presents a methodological framework to overcome data limitations concerning not only the hydrological fluxes but also the management rules of the water-related infrastructure throughout a river basin. It is aimed at identifying key vulnerabilities linked to the mismatch between uncertain water supplies and demands. In particular, the lack of data is an obstacle to validating a water resources allocation model across the full range of hydrological variability. Therefore, the modeling framework aims to establish a lower bound for water resource vulnerability, by providing lower-bound estimates for supply variability and demands and by assuming a cooperative management of the basin's existing infrastructure. Vulnerabilities identified in that first step despite these best-case assumptions are likely to exist. They are then further explored through additional scenarios. Ideally, the lower bound should explicitly consider the role of a large-scale reservoir system in altering water flows and bridging the temporal mismatch between the high-flow and high-demand seasons, as well as the role of hydrological uncertainty in that management. It therefore has to consider a monthly time step and an explicitly stochastic management module.

The proposed framework contributes to a growing body of work in the management of coupled human and natural systems (e.g., Giuliani et al., 2016; Ng et al., 2011; Yaeger et al., 2014), which necessitates data on both the hydrological fluxes and their management. It is applied to the present situation of the Tigris-Euphrates (T-E) river basin to identify key water resource vulnerabilities in this unstable region. Indeed, the T-E was listed among the most risk-prone transboundary basins in the world before the 2004 invasion of Iraq (Yoffe et al., 2003). Since then, the basin has been engulfed by a series of conflicts that have had ramifications far beyond its hydrological boundaries. Climate change and drought (Gleick, 2014; Kelley et al., 2015) and also management of land and water resources (Barnes, 2009; De Châtel, 2014; Feitelson & Tubi, 2017) have been cited as potential destabilizing factors. This regional backdrop stresses the urgency of developing methodological frameworks that overcome the lack of data.

In the absence of detailed, high-quality data on the space and time variability of water flows, and the operation of the basin's infrastructure, several approaches have been proposed to describe the state of water resources in T-E. Some studies have compiled existing data sources to describe the state of the basin's water resources and provide recommendations regarding the challenges and opportunities ahead (Altinbilek, 2004; Al-Ansari, 2013; Beaumont, 1998; Frenken, 2009; Kibaroglu & Unver, 2000). They generally depict a situation where given the current development projects, especially GAP (Turkish for "Southeastern Anatolia Project") in Turkey, total water demand from riparian countries may soon exceed supply. This has prompted the application of modeling approaches to understand how water can be allocated among riparian countries. Many of these studies examine water allocation during a single year, with an annual time step (e.g., Kucukmehmetoglu & Guldmann, 2010; Mianabadi et al., 2015, 2014). Recognizing that the seasonal patterns of runoff and irrigation do not match, Ohara et al. (2011) perform a subannual water balance downstream of Turkey, using a simplified representation of reservoirs. Yet given Turkey's position as the basin's water tower, the storage capacity of its reservoirs, and its ambitious development plans for the upstream portions of T-E it controls (Beaumont, 1998; Kolars and Mitchell, 1991), a more detailed approach is needed to evaluate vulnerabilities associated with infrastructure development. This level of detail can be provided by basin-wide water balance analysis at a finer, monthly time step, considers both distributed hydrological fluxes and the management of a large-scale reservoir system.

The rest of this paper proceeds as follows. Section 2 proposes the methodological framework that combines Land Data Assimilation (LDA) and hydroeconomic optimization to overcome the lack of data and enumerates the key assumptions needed to establish a lower bound to vulnerability within the basin. Then, section 3 introduces the application of that framework to produce that lower bound in the T-E. Section 4 presents the key identified vulnerabilities in that scenario. Then, section 5 builds on these results to further investigate the near closure of the Euphrates portion of the basin. Finally, strengths and weaknesses of the framework vis à vis its case study application are discussed in the concluding section 6.

2. Framework: Building a *Best Case*

2.1. Vulnerability Modeling

By definition, vulnerability is a *measure of possible future harm* (Hinkel, 2011; Ionescu et al., 2009; Wolf et al., 2013). Here we are concerned with identifying key vulnerabilities in river basins in their current state, and the phrase *possible future harm* refers to the hypothetical character of the damage, contrary to damage that has already materialized in a past event. Using an analytical approach, Rougé et al. (2015) determined that to measure vulnerability in any given system, the following is necessary:

(i) Equations determining the dynamic of that system over time;
(ii) A management rule or the possibility to determine one;
(iii) A representation of variability in that system; and
(iv) A function assessing harm in a given state of that system.

In the case of water resources systems, the dynamics (i) are given by the water balance equation, which can be written for all nodes of the network representing the river system:

$$\boldsymbol{s}_{t+1} - \boldsymbol{C}^R(\boldsymbol{r}_t + \boldsymbol{l}_t) = \boldsymbol{s}_t + \boldsymbol{q}_t - \boldsymbol{e}_t - \boldsymbol{w}_t, \tag{1}$$

where $\boldsymbol{s}_t$ and $\boldsymbol{s}_{t+1}$ are the vector of reservoir storage at the beginning and end of the period, $\boldsymbol{r}_t$ and $\boldsymbol{l}_t$ are the vector of releases and spills, $\boldsymbol{q}_t$ are the inflows, $\boldsymbol{e}_t$ are the evaporation losses, and $\boldsymbol{w}_t$ is the net water consumption, that is, gross consumption minus return flows. $\boldsymbol{C}^R$ is the reservoir system connectivity matrix, where $\boldsymbol{C}^R_{j,k} = 1(-1)$ when reservoir j receives (releases) water from (to) reservoir k.

A water allocation policy (ii) and a representation of variability (iii), starting with hydroclimatic variability, are classic features of water resources modeling. As for (iv), common approaches to assessing harm in water resources systems include metrics associated with the nonrespect of a threshold or with failure to meet the integrality of the demand (Hashimoto et al., 1982) or economic valuations of water across space and time (Harou et al., 2009). Other ways can be imagined; it is worth noting that any evaluation of harm includes a normative choice (Hinkel, 2011; Rougé et al., 2015). In any case, knowledge about demands and about the thresholds existing in a water resources systems is necessary for assessing harm.

2.2. Missing Data and Key Assumptions

This work deals with identifying key vulnerabilities in a situation where data records are fragmentary or nonexistent regarding (ii) the allocation policy, (iii) hydroclimatic and other sources of variability, and (iv) the demands to meet. In this situation, it is difficult if not impossible to validate the tail ends of the probability distributions of model outcomes. Yet this is what is relevant to vulnerability assessments. Therefore, rather than accurately representing vulnerability, the modeling framework aims at obtaining a lower-bound estimate, through assumptions on (ii), (iii), and (iv). In other words, these assumptions aim at building a best-case scenario for the basin under consideration. The ultimate goal of this best-case scenario is to make sure that the resulting vulnerabilities identified while analyzing the results of that scenario are likely to exist. This is an important feature of the proposed framework as it makes it more difficult for riparian countries to challenge and contest the very existence of those vulnerabilities.

2.2.1. Best-Case Assumptions on Variability

Capturing hydroclimatic variability is necessary for vulnerability assessments. Best-case assumptions must limit the range of variability that is considered, for instance:

1. Only inflow variability is considered;
2. Long-term (e.g., multidecadal) variability is not considered.

The latter is due to the fact that uninterrupted long-term records are difficult to obtain in many data-scarce basins (see section 3.2 for the T-E). Considering long-term hydrological variations would greatly increase the range of considered inflow conditions (Koutsoyiannis, 2006; Koutsoyiannis & Montanari, 2007). The methodology for obtaining inflow data in data-scarce cases is detailed in section 2.3.

2.2.2. Best-Case Assumptions on Demand

Best-case assumptions minimize demand by only considering demand levels that can be modeled in the absence of reliable data:

1. Only irrigation demand is accounted for; this excludes industrial and domestic demand as well as ecological flows;
2. Deliveries can be obtained (see section 2.3), and deliveries are at most equal to the demands; they are lower if all demands are not met.

2.2.3. Best-Case Assumptions on the Allocation Policy

The allocation policy (ii) is closely related to the management of reservoirs, which have the ability to substantially alter water flow regimes. Large-scale multireservoir systems are often too complex to enable the parametrization of rule-based simulation models without substantial information on the reservoirs' purposes. This information is often unavailable, and it would be a challenge to try and calibrate operation policies using fragmentary hydrological flow records. What is more, flow regimes keep being altered by new reservoirs as they go online, which also incidentally causes the operating rules of existing reservoirs to keep changing. In this context, vulnerability-minimizing assumptions for reservoir management are the following:

1. A cooperative allocation strategy; and
2. The allocation strategy prioritizes meeting irrigation demands.

The latter reflects a context where riparian countries emphasize food security and is consistent with the fact that data on irrigation withdrawals reflect observed fluxes rather than actual irrigation demand. What is more, we are looking for demand deficit as a vulnerability indicator (see section 2.1).

Obtaining reservoir rules through optimization is an alternative where the high number of state and decision variables leads to the so-called *curse of dimensionality* (e.g., Pereira & Pinto, 1985), which constitutes an insurmountable obstacle for most algorithms. Stochastic dual dynamic programming (SDDP; Pereira, 1989) is one of the few solutions available for the optimization of large-scale reservoir systems and the production of sensible operating policies. It can be used even in situations where data availability on the system itself is limited (Rougé & Tilmant, 2016). Section 2.4 provides details on this methodology.

2.3. Land Data Assimilation

Process-based hydrological models, remote sensing, and LDA systems, which combine the two, can compensate for the lack of direct information on upstream hydrological fluxes (Bastiaanssen et al., 2000; Hrachowitz et al., 2013; Maswood & Hossain, 2016; Zhang et al., 2014). As shown by Kolars and Mitchell (1991) in the T-E, these flows are very difficult to evaluate in a context of fragmented institutions, weak governance, and politically motivated claims on the geographical origin of the water supply. Coupling remote sensing with a rule-based irrigation model can provide insights on such complex situations (Evans & Zaitchik, 2008).

Estimates of naturalized streamflow throughout the river system were extracted from simulations performed with the Noah Land Surface Model (Noah LSM; Ek et al., 2003) v3.2 within the NASA Land Information System (Kumar et al., 2006) software framework v6.1. Noah LSM is widely used in land surface modeling, including the North American Land Data Assimilation System (Mitchell et al., 2004) and the Global Land Data Assimilation System (Rodell et al., 2004), and is also used as the land component in weather forecasting models. It is selected for this application because of its advanced physics, widespread use, and flexible parameterization. These are the characteristics that a LSM would need to possess to be used for the framework presented in this work. The goal of this work is not to ascertain what the best LSM is in a given situation but to demonstrate how a suitable LSM can be a key piece to vulnerability assessments in data-scarce river basins. Naturalized estimates obtained through LDA are conceptually appropriate as input to a hydroeconomic model, which use them to output water management decisions concerning reservoir operations and irrigation withdrawals. Background information on Noah LSM can be found in supporting information section S2.

In addition to providing streamflow inputs for hydroeconomic modeling, Noah 3.2 was used to generate estimates of irrigated water demand as a function of meteorological conditions, cropping season length, and local soil properties. These estimates were generated by including an irrigation module in the model designed to simulate traditional flood irrigation (algorithm detailed in supporting information section S3.1; Yilmaz et al., 2014). This approach has been tested in previous simulations in the T-E basin (Evans & Zaitchik, 2008; Zaitchik et al., 2005) and the Nile Delta (Yilmaz et al., 2014).

2.4. Hydroeconomic Optimization Through SDDP

Water allocation in multipurpose multireservoir systems can be formulated as a nonlinear and stochastic multistage decision-making problem. The goal is to determine a sequence of optimal allocation decisions $\boldsymbol{x_t}$ that maximizes the expected benefits Z from system operation over a planning period time T, while meeting operational and/or institutional constraints:

$$\max_{\boldsymbol{x}_t}\{Z\} = \max_{\boldsymbol{x}_t}\left\{E\left[\sum_{t=1}^{T}\alpha_t b_t(\boldsymbol{s}_t,\boldsymbol{q}_t,\boldsymbol{x}_t) + \alpha_{T+1}v(\boldsymbol{s}_{T+1},\boldsymbol{q}_T)\right]\right\}, \tag{2}$$

where $b_t(\cdot)$ is the immediate benefit function at stage t, $v(\cdot)$ is the terminal value function, α_t is the discount factor at stage t, and $E[\cdot]$ is the expectation operator. The vector of allocation decisions $\boldsymbol{x}_t$ includes release $\boldsymbol{r}_t$, spill $\boldsymbol{l}_t$, storage $\boldsymbol{s}_{t+1}$, and water withdrawals $\boldsymbol{i}_t$. Immediate benefits $b_t(\cdot)$ include the net benefits from system generation and penalties for not meeting target demands and/or violating operational and/or policy constraints such as minimum flow requirements.

At stage t, the immediate benefit function $b_t(\cdot)$ can be written as follows:

$$b_t(\boldsymbol{s}_t, \boldsymbol{q}_t, \boldsymbol{r}_t) = \tau_t(\boldsymbol{\pi} - \theta)'\boldsymbol{P}_t - \xi'_t\boldsymbol{z}_t, \tag{3}$$

where τ_t is the number of hours in period t, $\boldsymbol{P}_t$ (MW) is the vector of power generated, $\boldsymbol{\pi}$ is the vector of energy price (\$/MWh), $\boldsymbol{\theta}$ is the vector of the operation and maintenance cost (\$/MWh), and $\boldsymbol{z}_t$ is the vector of deficits or surpluses (unit deficit or surplus) penalized by the vector ξ'_t of penalties (\$/unit deficit or surplus).

To provide a lower bound for vulnerability, including demand shortage, irrigation withdrawals are treated as constraints. Vector z_t includes irrigation deficits, that is, the differences between irrigation requirements and the amount of water effectively delivered to the farms:

$$\boldsymbol{z}_t^{\text{irr}} = \max(I_t - \varepsilon i_t, 0), \tag{4}$$

where I_t is the crop water requirement at stage t and ε is the irrigation efficiency.

Most solutions to these problems, including discrete stochastic dynamic programming, become intractable in large-scale systems where the computational effort increases exponentially with the number of state variables. Simulation-optimization alternatives such as Evolutionary Multi-Objective Direct Policy Search (Giuliani et al., 2016) are promising for exploring other aspects of system complexity but require significant computing power (Giuliani et al., 2017) and have not been tested for systems of more than four reservoirs. SDDP is an extension of stochastic dynamic programming that avoids this curse by decomposing the nonlinear multistage problem into a series of one-stage linear problems, enabling computation in a matter of hours without parallelization. This algorithm is based on the approximation of the expected cost-to-go functions by piecewise linear functions (hyperplanes). It is organized through an iterative procedure in which new hyperplanes are added to the regions of the state space where a quality approximation is most needed, that is, in the regions explored by the system (Tilmant & Kelman, 2007).

When data availability is limited, as is the case in this study, this algorithm has been shown to lead to results that can be difficult to validate and interpret, and a year-periodic reoptimization (YPRE) scheme has been proposed to overcome this difficulty (Rougé & Tilmant, 2016). The reoptimization can be used with any number of simulation time series. The resulting algorithm is called SDDP-YPRE in this work.

3. Application to the T-E

3.1. The T-E Basin

The Euphrates and Tigris rivers are two major rivers in western Asia, with a drainage area of 879,000 km^2. From their headwaters in Turkey, they run almost in parallel before they merge to form the Shatt al-Arab, which discharges into the Persian Gulf (Figure 1). The northern and eastern parts of the basin are mountainous, whereas the southeastern part essentially consists of the Mesopotamian plain. The basin is shared by six countries: Turkey, Syria, Iraq, Iran, Saudi Arabia, and Jordan—the latter two only encompass small, arid portions of the basin. Iran is riparian only to the Tigris, and the Iranian portion of the basin is mainly through the Karkheh and Karun river basins. The former joins the Tigris at the upstream end of the Lower Mesopotamia Marshes. The latter discharges directly into the Shatt al-Arab downstream of these marshes along the confluence of the Euphrates and the Tigris rivers and has been excluded from the study area for that reason. The marshes are system of interconnected wetlands that was once home to 250,000 Marsh Arabs, important wildlife and migratory wildlife species as well as unique freshwater ecosystems. Its size has been reduced dramatically since the First Gulf War, even though restoration efforts have recently been implemented (Richardson & Hussain, 2006).

The hydrological regime of the upstream portions of the basin is characterized by a high-flow season starting in December and culminating during a snowmelt spring period from April to June, when 70% of the annual discharge takes place. This is followed by a low-flow season starting in July. Turkey contributes up to 98% of the Euphrates runoff (Kolars & Mitchell, 1991), whereas Turkey and Iraq each contribute around half of the annual discharge of the Tigris river upstream of the Mesopotamia Marshes.

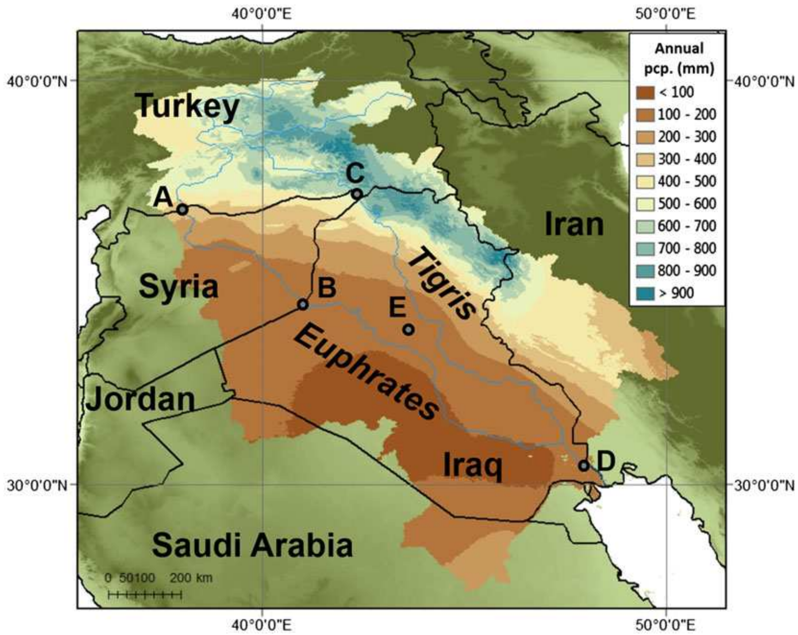

Figure 1. The Tigris-Euphrates river basin. Contours are annual average precipitation for the period 1982–2011. Points of interests for vulnerability identification (A–E) are as follows: (A) The Turkey-Syria border on the Euphrates, (B) the Syria-Iraq border on the Euphrates, (C) the Turkey-Iraq border on the Tigris, (D) the Tigris-Euphrates river basin's outlet, and (E) Tharthar Lake, a depression where excess waters are diverted in order to avoid flooding in Baghdad.

The Euphrates and Tigris rivers are key water resources for the riparian countries. Irrigated agriculture has been practiced since 6000 BCE in the Mesopotamia plain in present-day Iraq. More recently, several dams have been constructed during the second half of the twentieth century to harness hydropower potential in the headwaters of the basin's main rivers. These new impoundments also opened up new opportunities for using T-E waters for irrigation. The location of the infrastructure considered in this study, along with the water sources—lateral inflows—and sinks—consumption nodes and natural lakes—is given by an arc-node representation of the water network from Figure 2. This study considers the existing infrastructure in the basin, plus the Ilisu and Bekhme Dams (nodes 8 and 223, respectively), which are currently under construction.

Most developments in the Turkish portion of the T-E have taken place over the last four decades with the Southeastern Anatolia Project (GAP), an ambitious effort aimed at a total installed capacity of 7,256 MW and the irrigation of 1.7-million ha (Kolars & Mitchell, 1991). It most notably relies on the large elevation gradient along the course of the Euphrates river, where the three dams with the largest nominal hydropower production in the T-E basin are located; from upstream to downstream, these are Keban, Karakaya, and Ataturk (nodes 1 to 3). The latter also serves to irrigate large areas, including the Harran Plain (197) at the border with Syria. Syria also developed hydropower and irrigation during the second half of the twentieth century, organizing its development plans around the Tabqa Dam (101). Downstream, Iraq built one major dam on the Euphrates at Haditha (201) and on the Tigris at Mosul (221), but it also harnessed the potential of the Tigris affluents in the Zagros mountains (223, 227, 239, and 240). In addition, diversions meant to protect Iraqi cities from floods created and sustained artificial lakes in natural depressions, most notably Tharthar Lake (238; E in Figure 1), which protects Baghdad by receiving surplus Tigris flow. Finally, Iran also has built the Seymareh and Karkheh dams (300, 302) in the Karkheh river basin to exploit the available hydropower potential and develop irrigated agriculture.

3.2. Hydroclimatic Estimates

In this study, Noah 3.2 was implemented in uncoupled mode (i.e., not linked to a climate model), with meteorological forcing drawn from the NASA Modern-Era Reanalysis for Research and Applications (Rienecker et al., 2011) supplemented with Climate Hazards Group InfraRed Precipitation with Stations (Funk et al., 2015) satellite-derived precipitation estimates. Noah LSM requires a suite of gridded parameter fields to represent soil, vegetation, and land cover conditions. This work used the Food and Agriculture Organization of the United Nations (FAO) global soil data set, Moderate Resolution Imaging Spectrometer-derived estimates of vegetation fractional coverage, the U.S. Geological Survey global land cover map supplemented with Moderate Resolution Imaging Spectrometer-derived estimates of active irrigated land produced at 500-m resolution (Salmon et al., 2015), and the GTOPO (Global Topography) data set at 1-km resolution. Noah LSM simulations were performed at 5-km resolution. A 30-year spin-up was performed and the simulation was then run continuously for the period 1982–2011. Noah 3.2 was used to generate estimates of naturalized streamflow and irrigated water demand. The latter was obtained for 2001–2008 only, based on a map of irrigated areas circa 2004–2005 (Salmon et al., 2015).

Simulated annual average evapotranspiration estimates from irrigation were assessed by comparing simulated evapotranspiration in irrigated areas to satellite-derived evapotranspiration estimates derived using the Atmosphere Land Exchange Inverse algorithm (ALEXI; Anderson et al., 2007) implemented using Meteosat imagery (Yilmaz et al., 2014). ALEXI is a satellite-derived product that has not been independently validated for the T-E basin; therefore, we use the ALEXI estimates only as a check on model realism and not as a quantitative test of accuracy. We did not recalibrate the model to improve agreement with ALEXI. Note that these estimates

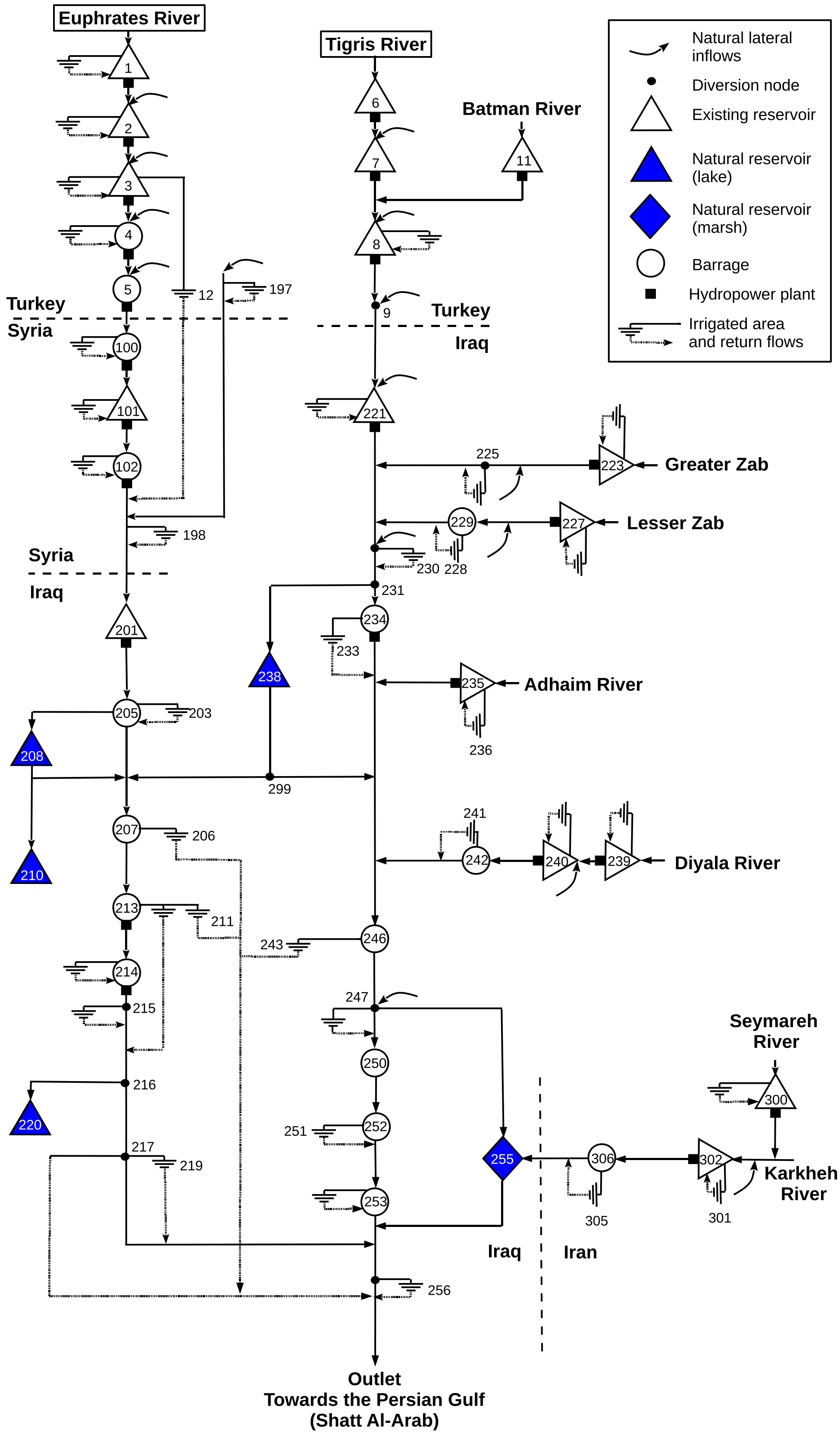

Figure 2. Network representation of the Tigris-Euphrates. Lists of hydropower and irrigation nodes are given in supporting information section S1.

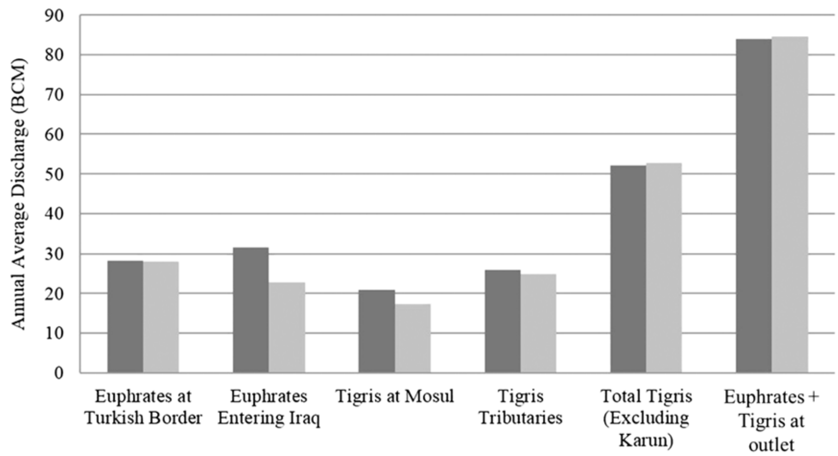

Figure 3. Average annual streamflow for the entire Tigris-Euphrates basin and points of interest within the basin. Dark bars are simulated naturalized discharge. Light bars are derived from available gauge records or previously published estimates.

apply only to on-field applications and return flows; losses in conveyance are not included in the Noah LSM simulations and were instead addressed by matching with basin-wide Food and Agriculture Organization of the United Nations estimates (see supporting information sections S3.2 and S3.3).

Calibrating naturalized streamflow estimates is challenging in the T-E, where the development of irrigation and the construction of large dams partly predates the 1982–2011 period included in our simulations. To address this challenge, we inventoried streamflow estimates available for Iraq in Saleh (2010) together with records from other countries in the basin provided by contacts in national water ministries. From these records we selected gauge records from upstream monitoring sites, located as close as possible to headwaters regions and upstream of all major modern irrigation developments. These records were assumed to represent approximately *natural* conditions and were used to bias correct simulated streamflow estimates. Recognizing that this is an imperfect approximation of natural conditions, as even headwaters regions may include some human modification, we did not apply any bias correction to subbasins in which the mean and interannual standard deviation of monthly streamflow was within 15% of gauged records for that month. For subbasins in which the simulations were biased by more than 15% in any calendar month, we applied a simple bias correction consisting of a linear additive correction for the mean and a ratio scaling for standard deviation. Since the vast majority of streamflow in the T-E basin is generated in headwaters regions, it was not necessary to bias correct incremental discharge contribution of downstream reaches.

The bias-corrected simulated discharge records were provided as water supply inputs to the hydroeconomic optimization model as monthly time series of estimated incremental streamflow at each model node. Summed simulated incremental streamflows across the entire basin and at critical locations within it are consistent with previously published estimates (Figure 3). Comparisons with observed discharge suffer from a number of caveats: The observations come from gauges that correlate with the gauges used in bias correction, the period of gauge records does not match the period of simulation for most rivers, gauge locations are not an exact match to the points of interest, and the naturalized discharge estimates of the simulation are not intended to be exactly comparable to gauge records—for example, the *Euphrates entering Iraq* gauge observation is highly affected by upstream withdrawals. For these reasons we consider the comparison to be a test of general realism and not a formal evaluation. In Figure 3, Euphrates entering Iraq, *Tigris at Mosul*, and *Tigris tributaries* (sum of Greater Zab, Lesser Zab, Diyala, and Adhaim) observations are from gauge records reported in (Saleh, 2010), with a time period that overlaps the simulation period. *Euphrates at Turkish Border*, *Total Tigris*, and *Euphrates + Tigris at outlet* are from historical gauge records reported in previous studies (Beaumont, 1998). These records capture a time of lower water withdrawal, so are expected to more closely resemble naturalized discharge, but they do not overlap the simulation period.

3.3. Best-Case Water Allocation in the T-E Basin

Inflows, evapotranspiration and return flows are obtained through LDA (section 3.2). The modeling framework uses LDA-obtained inflow time series to adjust a first-order periodic autoregressive model (1) that accurately

10.1029/2017WR021489

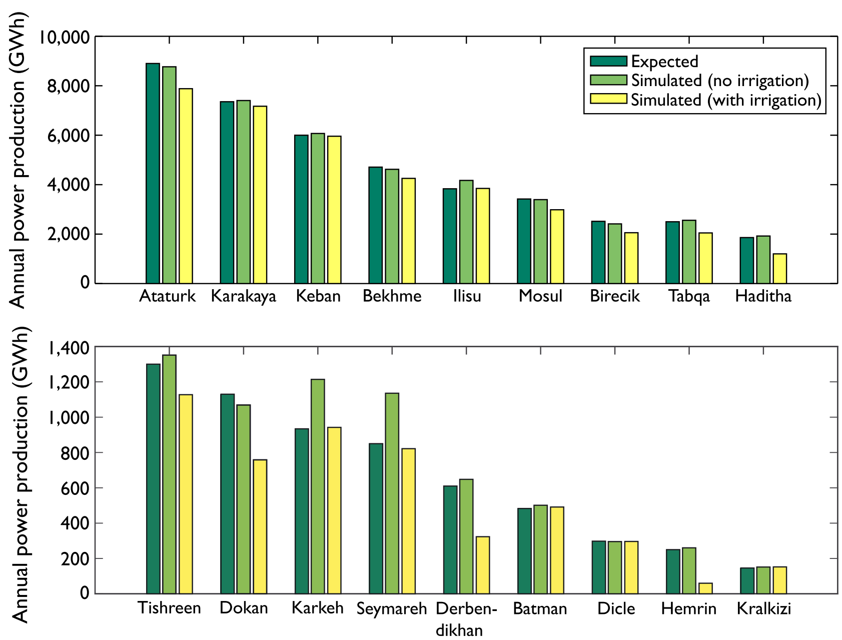

Figure 4. Expected versus simulated power production for the main reservoirs in this study.

captures the variability as well as the spatial and seasonal persistence of river discharges throughout the basin. This is consistent with the assumptions on variability from section 2.2.

Considering lag-1 persistence leads to having a hydrological state variable for each of the 28 lateral inflow nodes, adding to the 17 state variables that correspond to each of the reservoirs. Given the scale of this system, SDDP-YPRE (section 2.4; Rougé & Tilmant, 2016), implemented here as described in the reference provided, is one of the few available solutions to simulate the system's management. In this work, 1,000 monthly time series of 10 years each are used for the reoptimization, with the purpose of minimizing the influence of sampling error in analyzing the results. As a result, each run takes around 2 hr and 15 min to complete.

The characteristics of the reservoirs, run-of-river plants, and irrigation sites considered in this study can be found in the supporting information. The latter has been determined by using the monthly average of the 2001–2008 evapotranspiration and return flow estimates derived in section 3.2. Two additional steps, detailed in the supporting information (sections S3.3 and S3.4), are needed to transform these estimates into demand estimates. First, conveyance losses have to be estimated as a fraction of on-field application. Then, a distinction has to be made between withdrawals from water bodies hydrologically connected to the T-E and withdrawals from fossil aquifers that do not reduce T-E runoff but inject return flows into the network.

SDDP relies on the economic valuation of water for hydropower and irrigation requires that a monetary value be assigned to these uses. In the absence of data available throughout the river basin, those valuations rely on economic assumptions. Thus, the average energy price is assumed to be around 60 USD/MWh, which is the variable cost of a gas-fired power plant, a technology that is likely to be at the margin in the region. Irrigation being considered as a constraint in the model, unmet demands are penalized by a unit cost that far exceeds the value of water for hydropower.

3.4. Validation of the Best-Case Model

To ensure that the best-case basin model provides a lower bound to vulnerability, assumptions minimizing both variability and its impacts—with a lower bound on demand and a cooperative allocation—have been made in section 2.2. Yet the model's average behavior must also be validated .

The expected (or nominal) annual hydropower production is the only proxy that is available throughout the basin. It reflects both basin hydrology and the management of available water resources to productive ends. It is usually computed for feasibility studies for hydropower plants. Ideally, historical productions should

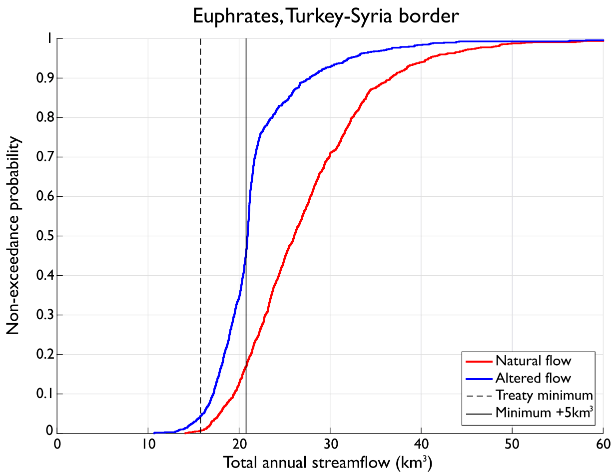

Figure 5. Impacts of infrastructure development on the probability distribution of annual flows at the border between Turkey and Syria on the Euphrates.

have been used instead, but they were not available for this study. Validation was conducted using averages of annual values for the last year of the 10-year reoptimized simulations, since the first years of those simulations are influenced by the initial storage conditions. It was performed using two scenarios, one assuming no-irrigation demand and another assuming full irrigation demand, because feasibility studies in the region tend to not account for how irrigation lowers the availability of water for hydropower, unless irrigation development predates dam construction.

Figure 4 compares nominal with average simulated productions for 16 of the 17 reservoirs in our model of the T-E basin—the expected production could not be found for the smallest, Al-Adhaim—and the two biggest run-of-river plants, Birecik (Turkey) and Tishreen (Syria). For both the full and no-irrigation scenarios, the same run produced the results for all reservoirs. Results from the no-irrigation scenario fall within 10% of the expected production for all reservoirs except two, confirming that feasibility studies were mostly done before developing irrigation. Differences may be attributed to limited data on the rule curves of the reservoirs, to climatic variability between 1982 and 2011 naturalized estimates and the period of reference for those studies and to the fact that feasibility studies ignored the potential impacts of all other developments upstream of these reservoirs.

The two exceptions are Seymareh and Karkheh, two recent reservoirs that came online in 2011 and 2001 in the Karkheh river basin in Iran. In both cases, results with irrigation match closely the expected production. Therefore, it is reasonable to assume that the development of irrigation may predate that of the feasibility studies.

The next section analyzes results from the full irrigation scenario.

4. Best-Case Scenario Results

Water allocation simulated with SDDP-YPRE and the assumptions from section 2.2 provides a lower bound on vulnerability. In that first scenario, there is enough water and reservoir storage to ensure over 99% reliability at all irrigation nodes on the main branches of the Tigris and Euphrates and 90% reliability in other branches (see supporting information section S3.4). Vulnerability identification focuses on border (section 4.1) and outlet flows (section 4.2).

4.1. Border Flows

The basin's vulnerability to low-flow years can be studied through the probability distribution of flows at key nodes in the river network, such as the crossing of national borders (A–C in Figure 1), for example, at the Turkey-Syria border on the Euphrates river (Figure 5). The comparison of natural and altered flows reveals the extent of upstream human interventions on the flow regime and the risks posed to downstream water users. In particular, two impacts are apparent in Figure 5, (1) irrigated agriculture and to a lesser extent, reservoir evaporation, significantly lower discharge, and (2) reservoir storage capacity reduces the variability of discharge on a year-to-year basis because it exceeds average annual flow.

This has an impact on the respect of international agreements/unilateral commitments such as the one in 1987 between Turkey and Syria, which stipulates minimum flow of 500 m^3/s or 15.75 km^3/year. So far and in this best-case scenario, infrastructure development upstream of these borders has only marginally increased the probability of not respecting the annual target, as it increased from 1% to 4% entering Syria (Figure 5). Yet downstream countries are vulnerable to an increase in upstream demand—due to irrigation—or a decrease in supply—due to climate change. Indeed, the current probability of being within 5 km^3 of the annual threshold is 44% at that border.

To further analyze the respective impacts of lower discharge and large storage capacity on border flows, we propose two metrics that compare the cumulative distribution functions (CDFs) of natural and altered flows—comparing empirical CDFs is being increasingly used to assess sensitivity (Chaney et al., 2015; Fenwick et al., 2014). On one hand, the difference in the average annual flow reflect the impacts of irrigation

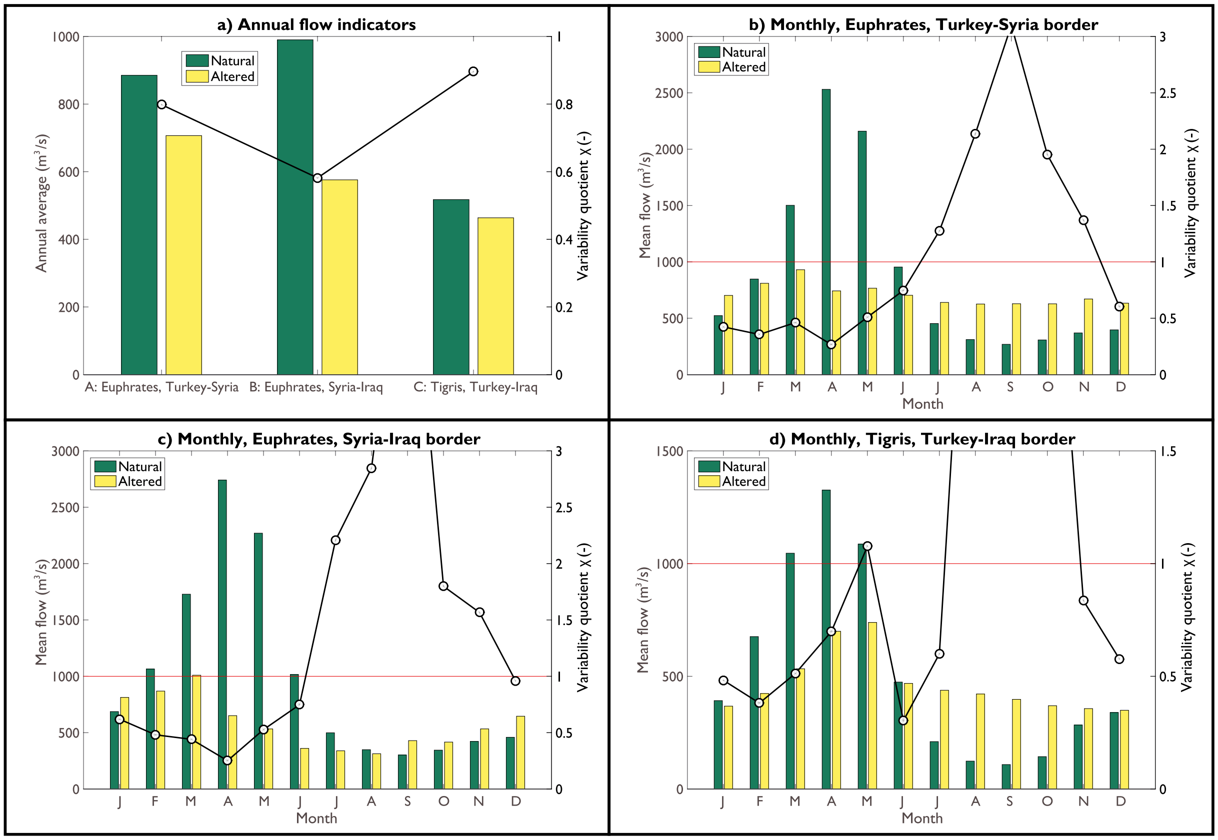

Figure 6. Average natural and altered annual and monthly flows and associated variability quotients *chi*, at the border crossings (A to C in Figure 1). Red lines signal $\chi = 1$, no change in variability.

(and reservoir evaporation). On the other hand, the following quotient χ compares the spread of natural and altered flows and, therefore, the impacts of storage on variability:

$$\chi = \frac{\int_0^\infty |F_a(x) - \mathbb{1}(x > \bar{a})|}{\int_0^\infty |F_n(x) - \mathbb{1}(x > \bar{n})|}, \tag{5}$$

where a and$n$ refer to altered and natural flows, respectively; $\bar{a}$ and $\bar{n}$ are their means; F is the CDF, and $\mathbb{1}$ is the characteristic function with values 1 if the condition that defines it is met and 0 otherwise. These two impacts mirror those of development on annual flows at all three borders in the T-E basin (Figure 6a). Impacts are largest at the Syria-Iraq border on the Euphrates, where little natural runoff is added compared to the Turkey-Syria border upstream compared with the additional irrigation withdrawals, amounting to a 42% reduction from the natural flow average. What is more, additional storage capacity in Syria (Tabqa Dam, node 101) adds to the flow regulation capacity, lowering χ from 0.80 to 0.58. Development of the Tigris side in Turkey has comparatively minimal impact on annual flow variability ($\chi = 0.90$) and reduced discharge (10%).

When it comes to monthly flows (Figures 6b–6d), the effects of storage on altered flows become apparent on both the mean flows and the variability quotients χ. Across all three border crossings, reservoirs store water during the snowmelt season (March to June) to release it for hydropower generation and downstream irrigation during the summer. Variability is suppressed ($\chi < 1$) as reservoirs refill, with the exception of panel (d) where there is too little upstream storage on the Tigris in Turkey to dampen variability in June. It is enhanced ($\chi > 1$) as they empty, adjusting downstream releases according to whether this is a dry or wet year. Thus, reservoirs also are a positive externality for downstream countries, since they store excess water during wet months (and years) to release it when demand for irrigation is highest with respect to natural supply, in summer months (and in dry years). Yet the weak difference in summer flows at the Syria-Iraq border on the Euphrates shows that upstream irrigation is depleting water availability downtream.

10.1029/2017WR021489

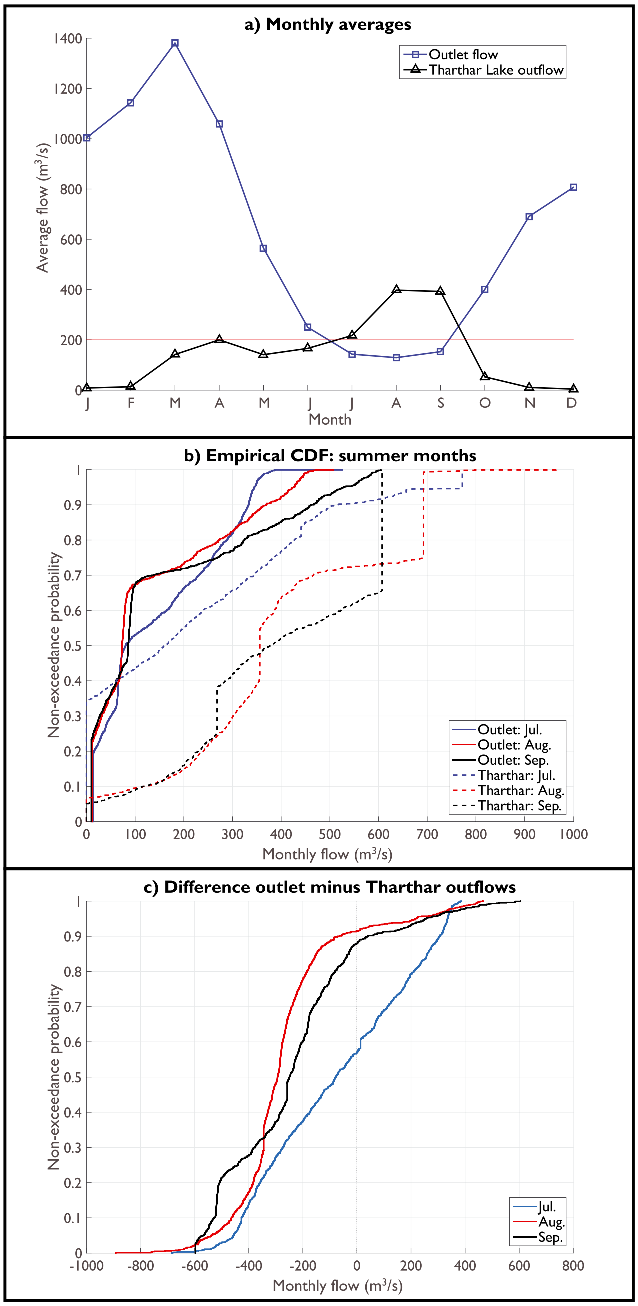

Figure 7. Comparison of outlet flows with outflows from Tharthar Lake.

4.2. Outlet Flows

The baseline best-case run also allows us to identify the precariousness of the current situation of the basin during summer months. Indeed, Figure 7 shows that then, flows from the basin outlets—both Shatt Al-Basra and Shatt al-Arab (256 in Figure 2, D in Figure 1)—are significantly lower than outflows from Tharthar Lake (E in Figure 1), a regulated lake set in a depression in central Iraq (Sissakian, 2011). This indicates that without this large (86 km^3 of storage) storage facility, there could be a supply deficit in on the Euphrates side where almost all Tharthar outflows go in our simulations. This use of Tharthar Lake waters for irrigation in the Euphrates basin is documented in the literature where it is branded as problematic because of the lake's high salinity (Beaumont, 1998; Rahi & Halihan, 2010). Note that these references only report these water transfers but do not prove that they might be needed to meet water demands.

Another indication that the basin is closing in summer months is that for at least 20% of the July to September months, outlet flows are equal to the return flow from the most downstream irrigation node. These outlet flows distributions are simulated assuming coordinated basin-wide management aimed at satisfying all irrigation demands. In reality, it is likely that demands are not fully met during dry years, leading to higher outlet flows. Yet this does not change the diagnosis that demands are close to or greater than supply in summer months, and it is coherent with observation that outlet flows are dwindling (Abdullah et al., 2015).

5. Results: Additional Scenarios

The previous section identified two key vulnerabilities on the Euphrates side of the basin. On one hand, there is a sensitivity of Euphrates flows at the Turkey-Syria border (A in Figure 1) to supply-demand changes, which might affect downtream flow availability, and specifically the ability of Turkey to meet its minimum flow commitment. On the other hand, downstream irrigation demands on the Euphrates side are dependent on transfers of saline water.

Building on the baseline scenario, noted A0 from now on, additional scenarios are explored (Table 1). In one set of scenarios, additional irrigation demands are created in Turkey (nodes 3 and 4 in Figure 2) in the Euphrates side of the basin—still well below the provisional irrigation totals if all of the planned irrigation developments come online in that area (Kolars & Mitchell, 1991; Tilmant & Kelman, 2007). Those scenarios are noted A. Note that these are net demand increases, that take return flows into account. In a second set of scenarios, the network is amended by deleting the link betzeen nodes 238 and 299 in Figure 2 so that Tharthar Lake has no outlet. Those scenarios are noted B. Note that all scenarios are run with

Table 1
Additional Scenarios

Water withdrawals	Baseline network	No Tharthar outlet (link 238–299)
Baseline irrigation at nodes 3–4	A0	B0
+1-km^3 net irrigation at nodes 3–4	A1	B1
+2-km^3 net irrigation at nodes 3–4	A2	B2
+3-km^3 net irrigation at nodes 3–4	A3	B3

Note. Node numbers refer to the network from Figure 2.

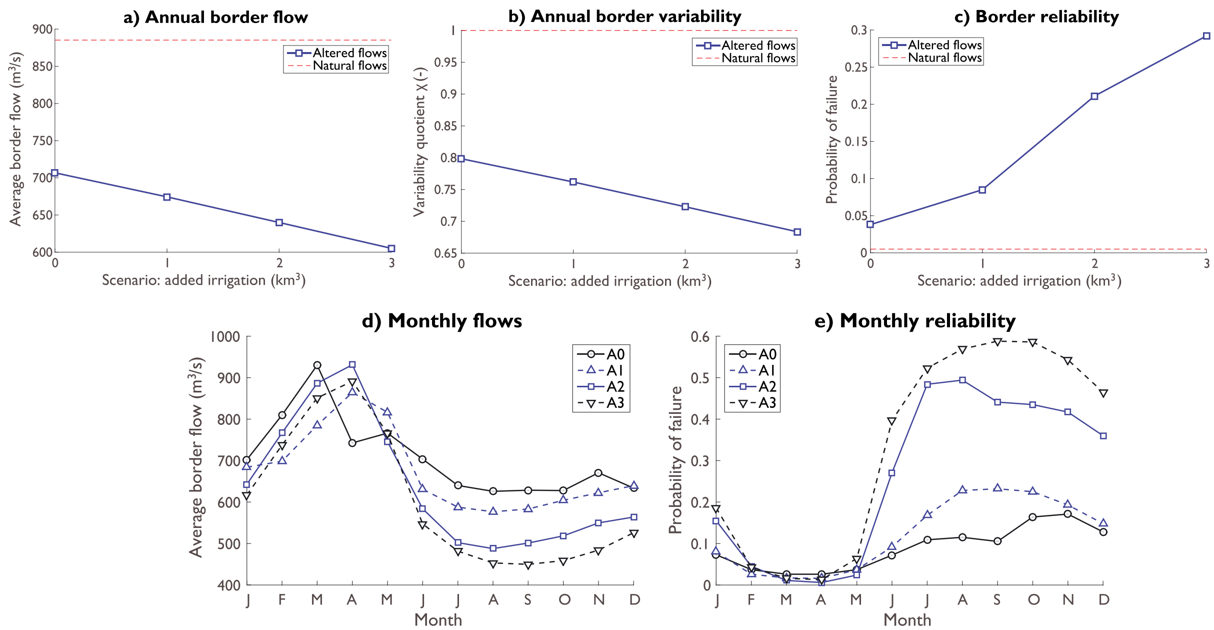

Figure 8. (a–e) Euphrates flow indicators at the Turkey-Syria border, and their sensitivity to increased irrigation in Turkey.

SDDP-YPRE using the same vulnerability-minimizing assumptions as A0, and simulation results feature the same 1,000 time series that are 10-year long with a monthly time step.

Section 5.1 investigates impacts of type A scenarios on border flows, then section 5.2 investigates impacts of type B scenarios on irrigation shortages in the Euphrates, which reflects this part of the basin's dependence on saline water transfers. Finally, section 5.3 compares all scenarios with basin-wide Euphrates side metrics and historical flows.

5.1. Sensitivity to Additional Irrigation (Scenarios A)

Impacts of Turkey demand increases on Euphrates border flows are summarized in Figure 8. Average annual flows decrease in a manner that matches the additional withdrawals (panel a), and since storage capacity stays the same, it becomes easier to store smaller quantity of waters in wet years and keep them for dry years, which lowers χ (panel b). Concerning the reliability of meeting treaty obligations, the sensitivity to supply-demand changes suggested by Figure 5 is confirmed (panel c), with the nonrespect probability jumping from 4% to almost 30% from A0 to A3. Dry season flows are those that suffer the most from decreased water availability (panels d and e), suggesting that the reliance of downstream irrigation on saline water transfers during

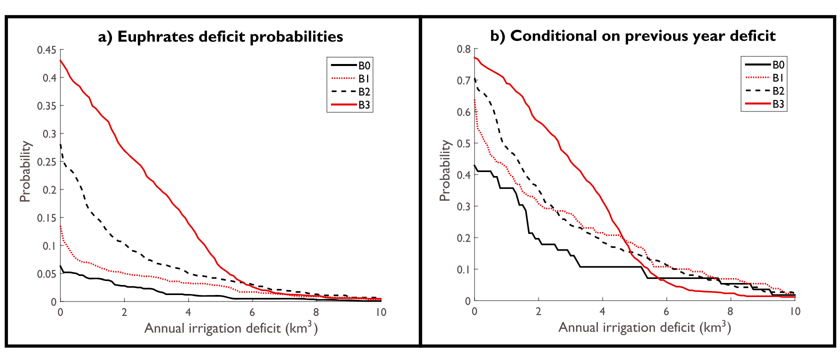

Figure 9. Exceedence probabilities of irrigation demand shortages in the whole Euphrates basin, under scenarios B0 to B3 (no saline water transfers). (a) Probabilities on a given year and (b) probabilities conditional on shortage the previous year.

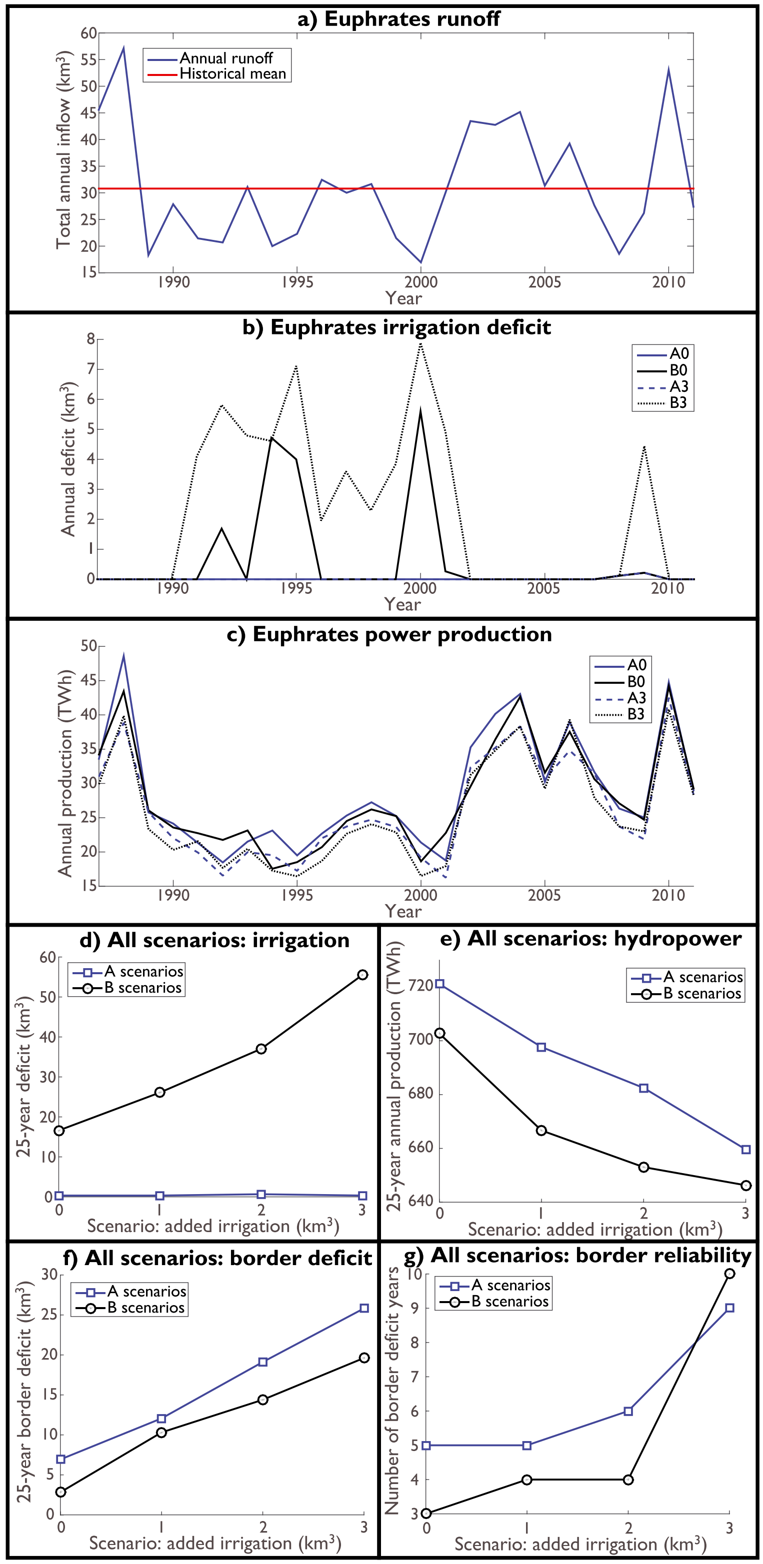

Figure 10. Results for the whole Euphrates basin, from reoptimization using the cuts (benefits-to-go functions) obtained from running SDDP-YPRE in each scenario defined in Table 1, with historical flows 1982–2011. Only 1987–2011 is shown to leave out the warmup period.

summer months would be increased by supplemental irrigation developments. Further investigation of this is the focus of type B scenarios.

5.2. Euphrates Dependence on Saline Water (Scenarios B)

Irrigation shortages in type B scenarios are better interpreted as reliance on saline water transfers. Figure 9a confirms the sensitivity of downstream irrigation to new irrigation developments in the Turkish portion of the Euphrates. Note that the average deficit (on all 1,000 simulations) roughly doubles in each scenario, from 0.15 km^3 in B0, to 0.32 km^3 (B1), 0.63 km^3 (B2), and 1.31 km^3 for scenario B3. This is not proportional to the increases in upstream irrigation demand across these scenarios. What is more, panel (b) results from Figure 9 suggest that irrigation deficits tend to be clustered in consecutive years. Both results demonstrate the relevance of accounting for storage and variability at a monthly time step over multiple years, instead of an (average) annual balance model over a single year.

5.3. Historical Comparisons

We applied the cuts (benefits-to-go functions) obtained from running SDDP-YPRE in each scenario to the whole historical streamflow record described in section 3.2, and used the 25 last years of those simulations (after a five-year warmup period) to investigate several metrics across scenarios in the whole Euphrates portion of the basin (Figure 10). The 2007–2009 drought was the only time the Khabur node 197—the only node not directly connected to the main course of the Euphrates in our model (Figure 2), while also at the epicenter of that drought—saw a water shortage in all scenarios. Yet the chronology of panels (a) to (c) suggests that this drought was not exceptional for the Euphrates flows, an observation corroborated by Eklund & Thompson (2017) who report an actual greening of areas irrigated by the main branch of the Euphrates during that 2007–2009 drought period, including in the Harran Plain (node 12). At any rate, that drought was short compared to a series of average-to-below-average years during the 1990s, which have more severe impacts both on the reliance on saline water transfers (type B scenarios on panel c), and on hydropower production (panel b). Given that irrigation areas are based on maps circa 2004–2005 (section 3.2), this poses the question whether irrigation developments between 2000 and the drought (Eklund & Thompson, 2017) created a scarcity situation that may been felt less acutely in the 1990s, when demands were lower. Panels (d) to (g) show 25-year aggregated results across all eight scenarios and demonstrate the sensitivity of all four displayed indicators on supplementary irrigation developments in Turkey.

6. Discussion and Conclusions

There is a consensus in the water community that cooperation on the management of transboundary water resources is both desirable and sometimes urgently needed. It is desirable to ensure the economic development and stability of a region; it is urgently needed in river basins experiencing closure where downstream riparian countries are vulnerable to unilateral management actions taken by their upstream neighbors. Not surprisingly, the most difficult situation is found in closing or closed transboundary river basins where basic cooperation, such as the exchange of hydrologic data, does not take place. In that case, downstream riparian countries can turn to quantitative modeling methods to anticipate future supplies. These methods can enable them to detect and quantify upstream interventions and then assess their downstream impacts.

This paper illustrates the use of such quantitative methods to identify key vulnerabilities in a data-scarce, politically unstable river basin: the Tigris-Euphrates. Using state-of-the-art remote sensing and hydrologic and hydroeconomic modeling, along with a set of appropriate assumptions, best-case vulnerabilities to changes in the flow regime due to irrigation withdrawals and reservoir storages are quantified. The very existence of the identified vulnerabilities is therefore more difficult to challenge by any riparian country, regardless of its position in the basin.

When applied to the T-E, the method points to two key vulnerabilities on the Euphrates side of the basin: (i) cross-border flows at the Turkey-Syria border are vulnerable to changes in storage in the Turkish reservoirs and (ii) irrigation schemes in Iraq are dependent on transfers of saline water from the Thartar lake. How these vulnerabilities should be addressed is beyond the scope of this manuscript. Rather, the proposed method is limited to their (hopefully uncontested) identification and quantitative assessment. This in turn, provides a factual basis regarding the status of the basin and (hopefully) should clear up the political space of unsubstantiated narratives.

Due to the limited space available, the analysis is presented for one infrastructure network (supplies and demands) corresponding to the current situation in the basin. Such analysis would certainly be enriched if carefully constructed scenarios representing potential futures were investigated with the proposed approach. This approach also does not explicitly consider water quality problems, for example, salinity, even though these are often present when water resources are being overexploited. For instance, in the T-E, current very low summer discharge in the Shatt al-Arab has been found to lead to saline intrusion as far as 92 km inland (Abdullah et al., 2016).

Acknowledgments
The work was supported by a project from the Food and Agriculture Organization titled "Support Cooperation on Agricultural Water Resource Management in the Lower Mesopotamia (Tigris and Euphrates)" and funded by the Government of Italy. We also would like to thank the Editor Ximing Cai, the Associate Editor, and two anonymous reviewers, as well as Simona Denaro whose comments have greatly improved this paper. This study is an independent assessment commissioned by the Food and Agriculture Organization of the United Nations (FAO). It does not represent the views of any riparian country or of the FAO. Besides infrastructure data contained in the supporting information, the hydroclimatic data used for LDA are available at the open-source repositories cited in section 3.2 and at the Global Runoff Data Centre (GRDC; data publicly availble as well). Results analyzed in section 4 are publicly available alongside the code used to generate them, at https://github.com/charlesrouge/Tigris-Euphrates. For additional queries, please contact Amaury Tilmant at the email address amaury.tilmant@cgi.ulaval.ca.

References

Abdullah, A. D., Gisen, J. I. A., van der Zaag, P., Savenije, H. H. G., Karim, U. F. A., Masih, I., & Popescu, I. (2016). Predicting the salt water intrusion in the Shatt al-Arab estuary using an analytical approach. *Hydrology and Earth System Sciences*, *20*(10), 4031–4042. https://doi.org/10.5194/hess-20-4031-2016

Abdullah, A. D., Masih, I., van der Zaag, P., Karim, U. F., Popescu, I., & Suhail, Q. A. (2015). Shatt al Arab River system under escalating pressure: A preliminary exploration of the issues and options for mitigation. *International Journal of River Basin Management*, *13*(2), 215–227. https://doi.org/10.1080/15715124.2015.1007870

Al-Ansari, N. A. (2013). Management of water resources in Iraq: Perspectives and prognoses. *Engineering*, *5*, 667–684. https://doi.org/10.4236/eng.2013.58080

Altinbilek, D. (2004). Development and management of the Euphrates-Tigris basin. *International Journal of Water Resources Development*, *20*(1), 15–33. https://doi.org/10.1080/07900620310001635584

Anderson, M. C., Norman, J. M., Mecikalski, J. R., Otkin, J. A., & Kustas, W. P. (2007). A climatological study of evapotranspiration and moisture stress across the continental United States based on thermal remote sensing: 1. Model formulation. *Journal of Geophysical Research*, *112*, D10117. https://doi.org/10.1029/2006JD007506

Barnes, J. (2009). Managing the waters of Ba'th country: The politics of water scarcity in Syria. *Geopolitics*, *14*(3), 510–530. https://doi.org/10.1080/14650040802694117

Bastiaanssen, W. G., Molden, D. J., & Makin, I. W. (2000). Remote sensing for irrigated agriculture: Examples from research and possible applications. *Agricultural Water Management*, *46*(2), 137–155. https://doi.org/10.1016/S0378-3774(00)00080-9

Beaumont, P. (1998). Restructuring of water usage in the Tigris-Euphrates basin: The impact of modern water management policies. *Yale F & ES Bulletin*, *103*, 168–186.

Chaney, N. W., Herman, J. D., Reed, P. M., & Wood, E. F. (2015). Flood and drought hydrologic monitoring: The role of model parameter uncertainty. *Hydrology and Earth System Sciences*, *19*(7), 3239–3251. https://doi.org/10.5194/hess-19-3239-2015

De Châtel, F. (2014). The role of drought and climate change in the Syrian uprising: Untangling the triggers of the revolution. *Middle Eastern Studies*, *50*(4), 521–535. https://doi.org/10.1080/00263206.2013.850076

Draper, S. E. (2007). Introduction to transboundary water sharing. *Journal of Water Resources Planning and Management*, *133*, 377–381.

Ek, M. B., Mitchell, K. E., Lin, Y., Rogers, E., Grunmann, P., Koren, V., et al. (2003). Implementation of Noah land surface model advances in the National Centers for Environmental Prediction operational mesoscale eta model. *Journal of Geophysical Research*, *108*(D22), 8851. https://doi.org/10.1029/2002JD003296

Eklund, L., & Thompson, D. (2017). Differences in resource management affects drought vulnerability across the borders between Iraq, Syria, and Turkey. *Ecology and Society*, *22*(4), 9. https://doi.org/10.5751/ES-09179-220409

Evans, J. P., & Zaitchik, B. F. (2008). Modeling the large-scale water balance impact of different irrigation systems. *Water Resources Research*, *44*, W08448. https://doi.org/10.1029/2007WR006671

Feitelson, E., & Tubi, A. (2017). A main driver or an intermediate variable? Climate change, water and security in the Middle East. *Global Environmental Change*, *44*, 39–48. https://doi.org/10.1016/j.gloenvcha.2017.03.001

Fenwick, D., Scheidt, C., & Caers, J. (2014). Quantifying asymmetric parameter interactions in sensitivity analysis: Application to reservoir modeling. *Mathematical Geosciences*, *46*(4), 493–511. https://doi.org/10.1007/s11004-014-9530-5

Frenken, K. (Ed.) (2009). *Irrigation in the Middle East region in figures—AQUASTAT survey 2008*. Rome: Food and Agriculture Organization of the United Nations. Chap. Euphrates-Tigris River Basin, pp. 63–71, FAO.

Funk, C., Peterson, P., Landsfeld, M., Pedreros, D., Verdin, J., Shukla, S., et al. (2015). The climate hazards infrared precipitation with stations—A new environmental record for monitoring extremes, *2*, 150066. https://doi.org/10.1038/sdata.2015.66

Geressu, R. T., & Harou, J. J. (2015). Screening reservoir systems by considering the efficient trade-offs—Informing infrastructure investment decisions on the Blue Nile. *Environmental Research Letters*, *10*(12), 125008.

Giuliani, M., & Castelletti, A. (2013). Assessing the value of cooperation and information exchange in large water resources systems by agent-based optimization. *Water Resources Research*, *49*, 3912–3926. https://doi.org/10.1002/wrcr. 20287

Giuliani, M., Castelletti, A., Pianosi, F., Mason, E., & Reed, P. M. (2016). Curses, tradeoffs, and scalable management: Advancing evolutionary multiobjective direct policy search to improve water reservoir operations. *Journal of Water Resources Planning and Management*, *142*(2), 04015050. https://doi.org/10.1061/(ASCE)WR. 1943-5452.0000570

Giuliani, M., Li, Y., Castelletti, A., & Gandolfi, C. (2016). A coupled human-natural systems analysis of irrigated agriculture under changing climate. *Water Resources Research*, *52*, 6928–6947. https://doi.org/10.1002/2016WR019363

Giuliani, M., Quinn, J. D., Herman, J. D., Castelletti, A., & Reed, P. M. (2017). Scalable multiobjective control for large-scale water resources systems under uncertainty. *IEEE Transactions on Control Systems Technology*, *18*(99), 1–8. https://doi.org/10.1109/TCST.2017.2705162

Gleick, P. H. (2014). Water, drought, climate change, and conflict in Syria. *Weather, Climate, and Society*, *6*(3), 331–340. https://doi.org/10.1175/WCAS-D-13-00059.1

Harou, J. J., Pulido-Velazquez, M., Rosenberg, D. E., Medellín-Azuara, J., Lund, J. R., & Howitt, R. E. (2009). Hydro-economic models: Concepts, design, applications, and future prospects. *Journal of Hydrology*, *375*, 627–643. https://doi.org/10.1016/j.jhydrol.2009.06.037

Hashimoto, T., Stedinger, J. R., & Loucks, D. P. (1982). Reliability, resiliency, and vulnerability criteria for water resource system performance evaluation. *Water Resources Research*, *18*(1), 14–20.

Hinkel, J. (2011). "Indicators of vulnerability and adaptive capacity": Towards a clarification of the science-policy interface. *Global Environmental Change*, *21*, 198–208.

Hrachowitz, M., Savenije, H., Blöschl, G., McDonnell, J., Sivapalan, M., Pomeroy, J., et al. (2013). A decade of predictions in ungauged basins (pub)—A review. *Hydrological Sciences Journal*, *58*(6), 1198–1255. https://doi.org/10.1080/02626667.2013.803183

Ionescu, C., Klein, R., Hinkel, J., Kumar, K. K., & Klein, R. (2009). Towards a formal framework of vulnerability to climate change. *Environmental Modelling and Assessment*, *14*(1), 1–16.

Kelley, C. P., Mohtadi, S., Cane, M. A., Seager, R., & Kushnir, Y. (2015). Climate change in the fertile crescent and implications of the recent Syrian drought. *Proceedings of the National Academy of Sciences*, *112*(11), 3241–3246. https://doi.org/10.1073/pnas.1421533112

Kibaroglu, A., & Unver, I. (2000). An institutional framework for facilitating cooperation in the Euphrates-Tigris River basin. *International Negotiation*, *5*(2), 311–330.

Kliot, N., Shmueli, D., & Shamir, U. (2001). Institutions for management of transboundary water resources: Their nature, characteristics and shortcomings. *Water Policy*, *3*(3), 229–255. https://doi.org/10.1016/S1366-7017(01)00008-3

Kolars, J. F., & Mitchell, W. A. (1991). *The Euphrates river and the Southeast Anatolia development project* (pp. 324). Carbondale, Illinois: Southern Illinois University Press.

Koutsoyiannis, D. (2006). Nonstationarity versus scaling in hydrology. *Journal of Hydrology*, *324*, 239–254.

Koutsoyiannis, D., & Montanari, A. (2007). Statistical analysis of hydroclimatic time series: Uncertainty and insights. *Water Resources Research*, *43*, W05429. https://doi.org/10.1029/2006WR005592

Kucukmehmetoglu, M., & Guldmann, J.-M. (2010). Multiobjective allocation of transboundary water resources: Case of the Euphrates and Tigris. *Journal of Water Resources Planning and Management*, *136*(1), 95–105.

Kumar, S., Peters-Lidard, C., Tian, Y., Houser, P., Geiger, J., Olden, S., et al. (2006). Land information system: An interoperable framework for high resolution land surface modeling. *Environmental Modelling & Software*, *21*(10), 1402–1415. https://doi.org/10.1016/j.envsoft.2005.07.004

Maswood, M., & Hossain, F. (2016). Advancing river modelling in ungauged basins using satellite remote sensing: The case of the Ganges–Brahmaputra–Meghna basin. *International Journal of River Basin Management*, *14*(1), 103–117. https://doi.org/10.1080/15715124.2015.1089250

McCaffrey, S. (2001). The contribution of the UN convention on the law of the non-navigational uses of international watercourses. *International Journal of Global Environmental Issues*, *1*, 250–263.

Mianabadi, H., Mostert, E., Pande, S., & van de Giesen, N. (2015). Weighted bankruptcy rules and transboundary water resources allocation. *Water Resources Management*, *29*(7), 2303–2321. https://doi.org/10.1007/s11269-015-0942-x

Mianabadi, H., Mostert, E., Zarghami, M., & van de Giesen, N. (2014). A new bankruptcy method for conflict resolution in water resources allocation. *Journal of Environmental Management*, *144*, 152–159. https://doi.org/10.1016/j.jenvman.2014.05.018

Mitchell, K. E., Lohmann, D., Houser, P. R., Wood, E. F., Schaake, J. C., Robock, A., et al. (2004). The multi-institution North American Land Data Assimilation System (NLDAS): Utilizing multiple GCIPs products and partners in a continental distributed hydrological modeling system. *Journal of Geophysical Research*, *109*, D07S90. https://doi.org/10.1029/2003JD003823

Molle, F., Wester, P., Hirsch, P., Jensena, J., Murray-Rust, H., Paranjpye, V., et al. (2007). *Water for food, water for life: A comprehensive assessment of water management in agriculture* (pp. 585–624), Chapter 16: River basin development and management. London: Earthscan and Colombo: International Water Management Institute.

Ng, T. L., Eheart, J. W., Cai, X., & Braden, J. B. (2011). An agent-based model of farmer decision-making and water quality impacts at the watershed scale under markets for carbon allowances and a second-generation biofuel crop. *Water Resources Research*, *47*, W09519. https://doi.org/10.1029/2011WR010399

Ohara, N., Kavvas, M. L., Anderson, M. L., Chen, Z. Q. R., & Yoon, J. (2011). Water balance study for the Tigris-Euphrates River Basin. *Journal of Hydrologic Engineering*, *16*(12), 1071–1082. https://doi.org/10.1061/(ASCE)HE.1943-5584.0000209

Olsson, O., Gassmann, M., Wegerich, K., & Bauer, M. (2010). Identification of the effective water availability from streamflows in the Zerafshan river basin, central Asia. *Journal of Hydrology*, *390*, 190–197.

Pereira, M. (1989). Optimal stochastic operations scheduling of large hydroelectric systems. *International Journal of Electrical Power & Energy Systems*, *11*(3), 161–169. https://doi.org/10.1016/0142-0615(89)90025-2

Pereira, M. V. F., & Pinto, L. M. V. G. (1985). Stochastic optimization of a multireservoir hydroelectric system: A decomposition approach. *Water Resources Research*, *21*(6), 779–792.

Rahi, K. A., & Halihan, T. (2010). Changes in the salinity of the euphrates river system in Iraq. *Regional Environmental Change*, *10*(1), 27–35. https://doi.org/10.1007/s10113-009-0083-y

Richardson, C. J., & Hussain, N. A. (2006). Restoring the garden of Eden: An ecological assessment of the marshes of Iraq. *BioScience*, *56*(6), 477–489.

Rienecker, M. M., Suarez, M. J., Gelaro, R., Todling, R., Bacmeister, J., Liu, E., et al. (2011). MERRA: NASA's Modern-Era Retrospective Analysis for Research and Applications. *Journal of Climate*, *24*(14), 3624–3648. https://doi.org/10.1175/JCLI-D-11-00015.1

Rodell, M., Houser, P. R., Jambor, U., Gottschalck, J., Mitchell, K., Meng, C.-J., et al. (2004). The global land data assimilation system. *Bulletin of the American Meteorological Society*, *85*(3), 381–394. copyright - Copyright American Meteorological Society Mar 2004; CaractÃl'ristique du document - Tables; Maps; Illustrations; DerniÃl're mise Ãă jour - 2017-11-10; CODEN - BAMIAT.

Rougé, C., Mathias, J.-D., & Deffuant, G. (2015). Vulnerability: From the conceptual to the operational using a dynamical system perspective. *Environmental Modelling & Software*, *73*, 218–230. https://doi.org/10.1016/j.envsoft.2015. 07.018

Rougé, C., & Tilmant, A. (2016). Using stochastic dual dynamic programming in problems with multiple near-optimal solutions. *Water Resources Research*, *52*, 4151–4163. https://doi.org/10.1002/2016WR018608

Saleh, D. K. (2010). Stream gage descriptions and streamflow statistics for sites in the Tigris River and Euphrates River basins Iraq (Tech. Rep.) United States: USGS.

Salmon, J., Friedl, M. A., Frolking, S., Wisser, D., & Douglas, E. M. (2015). Global rain-fed, irrigated, and paddy croplands: A new high resolution map derived from remote sensing, crop inventories and climate data. *International Journal of Applied Earth Observation and Geoinformation*, *38*, 321–334. https://doi.org/10.1016/j.jag.2015.01.014

Sissakian, V. K. (2011). Genesis and age estimation of the Tharthar depression, central West Iraq. *Iraqi Bulletin of Geology and Mining*, *7*(3), 47–62.

Tilmant, A., & Kelman, R. (2007). A stochastic approach to analyze trade-offs and risks associated with large-scale water resources systems. *Water Resources Research*, *43*, W06425. https://doi.org/10.1029/2006WR005094

Tilmant, A., & Kinzelbach, W. (2012). The cost of noncooperation in international river basins. *Water Resources Research*, *48*, W01503. https://doi.org/10.1029/2011WR011034

Timmerman, J. G., & Langaas, S. (2005). Water information: What is it good for? The use of information in transboundary water management. *Regional Environmental Change*, *5*(4), 177–187. https://doi.org/10.1007/s10113-004-0087-6

Watkins, K. (2006). Human development report. Beyond scarcity: Power, poverty and global water crisis (Tech. Rep.) New York, USA: United Nations Development Programme.

Wolf, A. T. (1999). Criteria for equitable allocations: The heart of international water conflict. *Natural Resources Forum*, *23*(1), 3–30. https://doi.org/10.1111/j.1477-8947.1999.tb00235.x

Wolf, S., Hinkel, J., Hallier, M., Bisaro, A., Lincke, D., Ionescuo, C., & Klein, R. J. T. (2013). Clarifying vulnerability definitions and assessments using formalisation. *International Journal of Climate Change Strategies and Management*, *5*(1), 54–70. https://doi.org/10.1108/17568691311299363

Wu, X., & Whittington, D. (2006). Incentive compatibility and conflict resolution in international river basins: A case study of the Nile basin. *Water Resources Research*, *42*, W02417. https://doi.org/10.1029/2005WR004238

Yaeger, M. A., Housh, M., Cai, X., & Sivapalan, M. (2014). An integrated modeling framework for exploring flow regime and water quality changes with increasing biofuel crop production in the U.S. Corn Belt. *Water Resources Research*, *50*, 9385–9404. https://doi.org/10.1002/2014WR015700

Yilmaz, M. T., Anderson, M. C., Zaitchik, B., Hain, C. R., Crow, W. T., Ozdogan, M., et al. (2014). Comparison of prognostic and diagnostic surface flux modeling approaches over the Nile River basin. *Water Resources Research*, *50*, 386–408. https://doi.org/10.1002/2013WR014194

Yoffe, S., Wolf, A. T., & Giordano, M. (2003). Conflict and cooperation over international freshwater resources: Indicators of basins at risk. *Journal of the American Water Resources Association*, *39*(5), 1109–1126.

Zaitchik, B. F., Evans, J., & Smith, R. B. (2005). MODIS-derived boundary conditions for a mesoscale climate model: Application to irrigated agriculture in the Euphrates basin. *Monthly Weather Review*, *133*(6), 1727–1743. https://doi.org/10.1175/MWR2947.1

Zhang, Y., Hong, Y., Gourley, J. J., Wang, X., Brakenridge, G. R., De Groeve, T., & Vergara, H. (2014). Impact of assimilating spaceborne microwave signals for improving hydrological prediction in ungauged basins. In V. Lakshmi, et al. (Eds.), *Remote sensing of the terrestrial water cycle* (pp. 439–450). Hoboken, NJ: John Wiley & Sons, Inc. https://doi.org/10.1002/9781118872086.ch27